

Equivalence of Stability Criteria for Multi-Fluid Stars

Tian-Shun Chen,^{1,*} Xiao-Ding Zhou,^{1,†} and Kilar Zhang^{1,2,3,‡}

¹*Department of Physics and Institute for Quantum Science and Technology, Shanghai University, Shanghai 200444, China*

²*Shanghai Key Lab for Astrophysics, Shanghai 200234, China*

³*Shanghai Key Laboratory of High Temperature Superconductors, Shanghai 200444, China*

We present a rigorous proof establishing the mathematical equivalence between two independent criteria for the marginal stability of multi-fluid relativistic stars: the dynamical criterion based on the vanishing of the fundamental radial pulsation mode's eigenfrequency, and the static criterion derived from the geometric alignment of mass and particle number gradients in the parameter space. Leveraging this equivalence, we introduce a powerful and computationally efficient framework as an upgraded version of the critical curve method, to systematically map the stability boundaries for multi-fluid mixed stars across the entire parameter space of central pressures. Our analysis, applied to a variety of nuclear and dark matter equations of state, reveals the existence of stable region in the observable mass-radius diagram. By resolving degeneracies with 3-dimensional Mass-Radius-Pressure diagrams, we provide a complete topological view of the ensemble. This work supplies a robust theoretical foundation for interpreting multi-messenger astronomical observations and constraining the properties of dark matter.

I. INTRODUCTION

The advent of multi-messenger astronomy has made compact stars as powerful laboratories for probing fundamental physics at the intersection of extreme gravity and high nuclear densities [1, 2]. A compelling theoretical frontier is the study of compact objects containing dark matter (DM), motivated by the potential for DM accretion over a star's lifetime [4, 5]. If assuming only gravitational interactions between DM and neutrons, the resulting DM-admixed neutron star (NS) is inherently a two-fluid mixed star system [19, 22]. Here we use the terminology “mixed star” for multi-fluid system where the components interact only through gravity, to distinguish from hybrid star [12] with other interactions besides gravitational ones. The stability for hybrid stars is summarized in [11]. Mixed stars are much more complicated to analyze than hybrid stars, since the latter have only one component for each layer, while the former is mixed inside. For DM-admixed NS, its structure and stability depend on a two-dimensional parameter space of central pressures, one for each component. The presence of DM could leave discernible imprints on the star's macroscopic properties, such as its mass-radius (M - R) relation, offering a novel window into the nature of DM [7, 8].

A prerequisite for any astrophysical model is dynamical stability. For multi-fluid mixed stars, two primary methods have been employed to identify the threshold of instability. The **Dynamical Method** is a rigorous perturbation analysis yielding a generalized eigenvalue problem, where marginal stability corresponds to the vanishing of the fundamental oscillation mode's (squared) frequency, $\omega_0^2 = 0$ [14, 15]. While definitive, this approach

is computationally intensive, limiting systematic explorations of the full parameter space.

In contrast, the **Static Method** offers a computationally efficient alternative, conjecturing that marginal stability occurs at points in the parameter space where the gradients of the total mass ($M = \sum_I M_I$, where M_I is the mass of fluid I) and particle numbers (N_I) are parallel: $\nabla M \parallel \nabla N_I$, for $\forall I$ [19]. This method relies solely on static equilibrium solutions, but its formal equivalence to the dynamical criterion has remained an unproven, foundational assumption.

In this work, we bridge this fundamental gap. Our primary contributions are threefold: First, we present a rigorous, first-principle proof of the mathematical equivalence between the dynamical ($\omega_0^2 = 0$) and static ($\nabla M \parallel \nabla N_I$) stability criteria. Second, basing on this validated static method, we perform a comprehensive stability analysis of DM admixed NS, as two-fluid applications, across the entire two-dimensional parameter space for a variety of realistic nuclear and DM equation of state (EoS). Third, we translate these theoretical stability boundaries into directly observable predictions by constructing stable region on the M - R plane and resolving degeneracies with 3-dimensional M - R - p^c (here p^c represents the central pressure) topological diagrams. This work provides a robust theoretical framework for interpreting multi-messenger observations, and to constrain the properties of DM by concerning the stability of compact stars.

II. THEORETICAL BACKGROUND

In this section, we review the fundamental theoretical framework for modeling the structure and stability of compact stars. For a standard single-component star, the stability against radial perturbations is determined by solving a Sturm-Liouville eigenvalue problem for the

* cts2003912@shu.edu.cn

† 18038288465@shu.edu.cn

‡ kilar@shu.edu.cn; Corresponding Author

squared oscillation frequencies, ω_n^2 [10, 13]:

$$\frac{d}{dr} \left(\Pi(r) \frac{du_n}{dr} \right) + [Q(r) + \omega_n^2 W(r)] u_n(r) = 0, \quad (1)$$

where the detailed forms of Π , Q and W can refer to [10, 13].

A star is dynamically stable if and only if the fundamental eigenvalue ω_0^2 is positive. We now generalize this framework to the more complex multi-fluid system.

The structure of \mathcal{N} -fluid mixed star is now described by a coupled set of TOV equations [24, 25], one for each component ($I = 1, 2, \dots, \mathcal{N}$) [26, 27]:

$$\frac{dm_I r}{dr} = \frac{4\pi r^2}{c^2} \varepsilon_I(r), \quad (2)$$

$$\frac{dp_I(r)}{dr} = - \frac{G(\varepsilon_I + p_I/c^2)(m_t + 4\pi r^3 p_t/c^2)}{r^2(1 - 2Gm_t/c^2 r)}, \quad (3)$$

where the gravitational source depends on the total mass $m_t = \sum_I m_I$, and total pressure $p_t = \sum_I p_I$. A unique solution is specified by a set of central pressures p_I^c , creating an \mathcal{N} -dimensional parameter space.

The stability analysis for this multi-fluid system is considerably more complex than solving the standard Sturm-Liouville problem of Eq. (1). However, the onset of instability still corresponds to a zero-frequency mode ($\omega_0^2 = 0$), which represents a static perturbation connecting adjacent equilibrium configurations. A crucial physical requirement is that this transformation must conserve the particle number N_I of each fluid. This leads to a powerful static criterion for marginal stability: the critical curve, which forms the boundary of the stable region, is identified by points in the parameter space where the contour of the conserved quantities—total mass M , particle numbers N_I —are tangent. Due to underlying thermodynamic relations, this geometric condition simplifies to requiring that the gradients of these three conserved quantities be parallel. This provides an efficient tool for mapping the stability boundary without the necessity of solving the full, coupled perturbation equations.

III. EQUIVALENCE OF THE DYNAMICAL AND STATIC STABILITY CRITERIA

In this section, we present the central theoretical result of our work by outlining the rigorous proof that establishes the equivalence between the dynamical and static criteria for marginal stability in multi-fluid relativistic stars. A more detailed derivation is collected in a companion paper [30], and here we illustrate the main derivation procedure as follows.

Step 1: Zero Modes and Parallel Condition

we begin by proving the following theorem

Theorem 1. *For an \mathcal{N} -fluid equilibrium configuration, the $\mathcal{N} + 1$ gradients, ∇M and ∇N_I ($I = 1, 2, \dots, \mathcal{N}$), are*

mutually parallel if and only if there exists at least one zero mode respect to radial perturbation.

Proof. For a certain static equilibrium configuration, when $\omega_n^2 = 0$ (or approaches 0^+) for some $n \in \mathbb{N}$ under radial perturbation, the corresponding eigenmode $\xi_{In}(r)e^{-i\omega_n t}$ becomes a quasi-static one: $\xi_{In}(r)$.

This mode corresponds to an infinitesimally slow transition between adjacent equilibrium states.

The radial oscillation equations are derived from perturbing $\nabla_\mu T_I^{\mu\nu} = 0$ and $\nabla_\mu J_I^\mu = \nabla_\mu (n_I u_I^\mu) = 0$. Here $T_I^{\mu\nu}$ is the energy momentum tensor, n_I is the particle number density and u_I^μ is the 4-velocity. We can further collect the currents in a unified form $J_{N_I}^\mu \equiv n_I u_I^\mu$, $J_{M_I}^\mu \equiv T_I^{\mu 0}$, and then the corresponding conserved charges are:

$$\begin{aligned} Q_{N_I} &\equiv - \int_{\Sigma} J_{N_I}^\mu a_\mu \sqrt{h} d^3x = N_I, \\ Q_{M_I} &\equiv - \int_{\Sigma} J_{M_I}^\mu a_\mu \sqrt{h} d^3x = M_I, \end{aligned} \quad (4)$$

where Σ is a spacelike hypersurface of fixed time, a_μ is the unit normal vector of Σ , h is the determinant of the induced 3-metric, and $\sqrt{h} d^3x$ is the invariant volume element on the 3-space. Q_i defined in this way is exactly the flux of J_i^μ through Σ . The above conservation conditions are the same for both static and disturbed situations, which ensures that the total mass M and particle number N_I are conserved in radial oscillations.

Therefore, at points $\vec{\sigma}^1$ in the parameter space with zero modes, M and N_I remain conserved along the direction that point to the adjacent point corresponding to the static solution, indicating extrema:

$$\frac{dM_{total}}{d\vec{\sigma}} = 0 \quad \text{and} \quad \frac{dN_I}{d\vec{\sigma}} = 0, \quad \text{for } \forall I, \quad (5)$$

which is equivalent to the parallelism of the gradients of M and N_I in the $\vec{\sigma}$ parameter space:

$$\nabla M \parallel \nabla N_I, \quad \text{for } \forall I. \quad (6)$$

□

Step 2: Variational Extremum Principle

The second part of the equivalence proof demonstrates that if any \mathcal{N} of the $\mathcal{N} + 1$ gradients ∇M and ∇N_I are parallel, then the remaining one is necessarily parallel to them as well. The detailed proof process of two-fluid case is listed in the appendix of the companion paper [30], which can be easily generalized to multi-fluid case. In this section, we present the main steps:

¹ what M and N_I depend on, and here we take $\vec{\sigma} = (p_1^c, p_2^c, \dots, p_{\mathcal{N}}^c)$, the central pressures for convenience.

Theorem 2. *A multi-fluid isentropic mixed star configuration satisfies the TOV equilibrium equations if and only if the total mass M is extremal with respect to all variations conserving all fluid particle numbers.*

Proof. Employing Lagrange multipliers, consider:

$$H[\vec{\sigma}] = M[\vec{\sigma}] - \sum_{I=1,2,\dots,\mathcal{N}} \lambda_I N_I[\vec{\sigma}]. \quad (7)$$

The theorem requires $\delta H = 0$ for arbitrary variations $\delta \varepsilon_I(r)$. Using the zero-temperature thermodynamic relation $\delta \varepsilon_I = \mu_I \delta n_I = (\varepsilon_I + p_I) \delta n_I / n_I$ (with μ_I the chemical potential) and transforming to energy density variations gives:

$$\begin{aligned} \delta H &= \delta M - \sum_I \lambda_I \delta N_I \\ &= \sum_I \int \left[\frac{\partial M}{\partial \varepsilon_I} \delta \varepsilon_I - \lambda_I \left(\frac{\partial N_I}{\partial \varepsilon_I} \delta \varepsilon_I + \sum_J \frac{\partial N_I}{\partial m_J} \delta m_J \right) \right] dr \\ &= 0 \quad (I, J = 1, 2, \dots, \mathcal{N}). \end{aligned} \quad (8)$$

If there exists λ_I that makes this equation hold, the stellar configuration must obey constraints [30]

$$\frac{\lambda_I n_I}{p_I + \varepsilon_I} = \text{const.} \quad \text{for } \forall I, \quad (9)$$

which make (8) eventually reduce to:

$$\frac{dp_I}{dr} = -(\varepsilon_I + p_I) \frac{m_{\text{total}} + 4\pi r^3 p_{\text{total}}}{r(r - 2m_{\text{total}})}, \quad \text{for } \forall I, \quad (10)$$

This is exactly one of the TOV equilibrium equations (3) and the theorem is proved. \square

The Lagrange multipliers can be arbitrarily rescaled (e.g., by dividing $\nabla M = \lambda_1 \nabla N_1 + \lambda_2 \nabla N_2$ by λ_1 or λ_2), ensuring the theorem's validity for any permutation of M and N_I . This permutation symmetry implies that if any \mathcal{N} of the $\mathcal{N} + 1$ gradients (∇M and ∇N_I) are parallel (indicating simultaneous extrema), the remaining one must also be parallel to them.

Physical Interpretation

In addition, stability can be displayed through the sign of the second-order variation of total mass M [14, 28, 50]:

- $\delta^2 M > 0 \Leftrightarrow \omega_0^2 > 0$: Stable
- $\delta^2 M = 0 \Leftrightarrow \omega_0^2 = 0$: Stability boundary
- $\delta^2 M < 0 \Leftrightarrow \omega_0^2 < 0$: Unstable

$\delta^2 M > 0$ means perturbations raise energy, needing external work (stable). $\delta^2 M < 0$ allows kinetic energy growth without external input (unstable).

IV. APPLICATIONS OF STABILITY METHODS WITH DIFFERENT EQUATIONS OF STATE

Armed with the rigorously proven equivalence of the stability criteria, we now apply the computationally efficient static method to systematically investigate the stability of DM-admixed NS. To ensure our conclusions are not limited to a specific model and to explore the impact of different microphysics, we test their universality by performing the stability analysis with various EoS for both the DM and NM components. We construct mixed star models by combining a selection of well-established EoS.

For DM, we consider two distinct theoretical models. The first one is a well-motivated free Fermi gas EoS [1],

$$\begin{aligned} \varepsilon &= \frac{1}{2\pi^2} \int_0^{k_F} dk k^2 \sqrt{k^2 + m_f^2}, \\ p &= \frac{1}{6\pi^2} \int_0^{k_F} dk \frac{k^4}{\sqrt{k^2 + m_f^2}}, \end{aligned} \quad (11)$$

where m_f is the fermion mass and k_F is the Fermi momentum. The second one is a self-interacting Φ^4 bosonic model [35, 36]:

$$\varepsilon = 3p + B_4 \varepsilon^{1/2}, \quad (12)$$

where the free parameter $B_4 = \frac{0.08}{\sqrt{\lambda_4}} \left(\frac{m_b}{\text{GeV}} \right)^2$. Here m_b is the boson mass and λ_4 is the coupling.

For NM, we utilize both the widely-used SLy4 EoS [31–33] and an analytical double-polytropic EoS obtained from holographic QCD [34]:

$$\varepsilon = 0.140 \mathcal{A}^{0.571} p^{0.429} + 3.896 \mathcal{A}^{-0.335} p^{1.335}, \quad (13)$$

where $\mathcal{A} = 1.8 \times 10^{-5} \times \ell^{-7}$, and ℓ represents the brane asymptotic separation.

We apply astrophysical units for these EoS: $r_\odot = G_N M_\odot / c^2$, $\varepsilon_\odot = M_\odot / r_\odot^3$, $p_\odot = c^2 \varepsilon_\odot$. For each EoS, the required particle number density n_i is derived from the fundamental thermodynamic identity at zero temperature.

In the literature, the common critical curve method [16–18] to obtain the boundary of stability is to find the contour tangent points of two fields and connecting them.

Here instead, we find an equivalent approach but with higher accuracy and computational efficiency. We map the stability boundaries by applying the static criterion ($\nabla M \parallel \nabla N_{\text{DM}} \parallel \nabla N_{\text{NM}}$) across the two-dimensional parameter space of central pressures, (p_1^c, p_2^c) . To precisely identify where the gradients become parallel, we compute the magnitude of the normalized cross product between them. For any two conserved quantities A and B, this metric is defined as:

$$\mathcal{C}_{A,B} \equiv |\hat{u}_{\nabla A} \times \hat{u}_{\nabla B}| \equiv \left| \frac{\nabla A}{|\nabla A|} \times \frac{\nabla B}{|\nabla B|} \right|. \quad (14)$$

A point lies on a critical curve of marginal stability when this quantity vanishes. Fig.1 displays a primary example: a heatmap of \mathcal{C}_{M,N_1} , the metric for total mass and the particle number of DM, for Fermionic DM with $m_f=0.5$ and SLy4 model. The dark valleys, where the cross product magnitude approaches zero, precisely trace out the critical curves where the squared oscillation frequencies ω_n^2 vanish for different radial modes. The valley represents the boundary of absolute stability, beyond which all configurations are dynamically unstable.

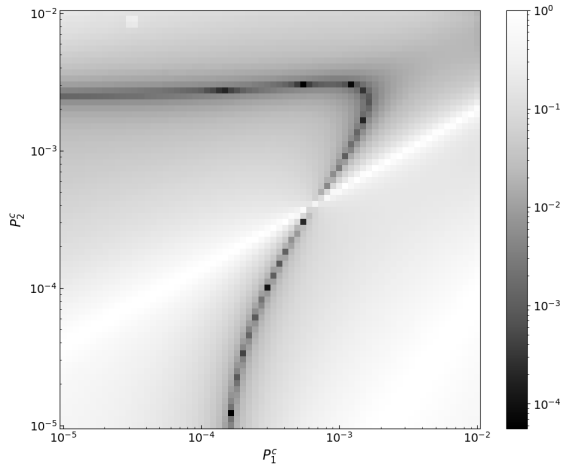


FIG. 1: Stability boundaries visualized via the normalized cross product of gradients as functions of central pressures, for Fermionic DM with (p_1^c) and SLy4 (p_2^c) model. Dark valleys indicate regions of marginal stability. Both the horizontal and vertical axes are in astrophysical units (p_\odot). The background black-and-white heatmap shows the absolute value for the cross product of the normalized gradient directions, at each point of the total mass field and DM particle number field. Darker colors indicate closer parallelism between the two fields' gradient directions.

Our result across different EoS combinations confirms the theoretically expected nested hierarchy of stability boundaries, while revealing a rich and robust topology, as shown in the companion paper [30]. Most notably, for all combinations of EoS tested, we find regions of parameter space where both central pressures are higher than their respective single-fluid critical pressures, yet the combined two-fluid system remains stable. This non-trivial emergent property of the gravitational coupling underscores the necessity of a full two-fluid analysis. The qualitative features and topological structure show similarity for different EoS, like that of a self-interacting bosonic DM (with $B_4 = 0.05$) and holographic NM (with $l^{-7} = 10300$) shown in Fig.2.

To explicitly demonstrate the power of our equivalence proof and to cross-validate our numerical implementation, we perform a direct calculation of the eigenfrequencies using the dynamical method for the selected star model in Fig.2. By solving the full coupled Sturm-

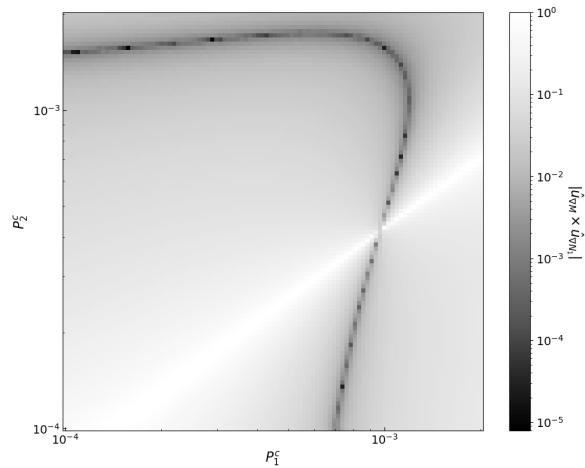


FIG. 2: Boundaries of the stable region for a two-fluid star composed of a self-interacting bosonic DM and holographic NM models. The parameters are defined the same way as in Fig.1.

Liouville system, we calculated the eigenvalue: squared frequency of the fundamental mode, ω_0^2 . As shown in Fig.3, the results are in perfect agreement within the numerical accuracy: the zero eigenvalue points coincide with the critical points predicted by the static criteria shown in Fig.2. Across these points, the sign of eigenvalue changes, indicating the transition between stable and unstable region. This numerical confirmation validates the accuracy and reliability of the static method for mapping the stability boundaries of two-fluid stars.

Besides, the numerical experiments clearly shows the efficiency of the critical curve method. It takes one hour on a normal desktop computer to generate Fig.2, while it costs about one week for Fig.3.

V. ASTROPHYSICAL IMPLICATIONS: STABLE REGION AND TOPOLOGICAL ANALYSIS

For two-fluid mixed stars, the stability boundaries mapped in the two-dimensional parameter space of central pressures provide a complete theoretical picture of stellar stability. However, to connect our theoretical findings to astrophysical observables, it is more convenient to project the identified stable regions onto the M - R plane. This mapping transforms the complicated stability criteria into concrete, testable predictions. Unlike single-fluid stars, which form a simple one-dimensional curve on the M - R plane, the stable two-fluid configurations occupy a contiguous two-dimensional region in the parameter space [16]. The projection of this stable region, $\Omega_{\text{stable}} = \{(p_{DM}^c, p_{NM}^c) | \omega_0^2 \geq 0\}$, results in a two-dimensional stable region:

$$\mathcal{I}_{\text{stable}} = \{(M, R) | \exists (p_{DM}^c, p_{NM}^c \in \Omega_{\text{stable}})\}. \quad (15)$$

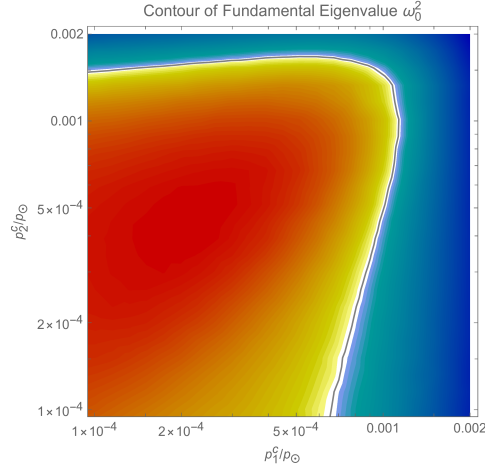
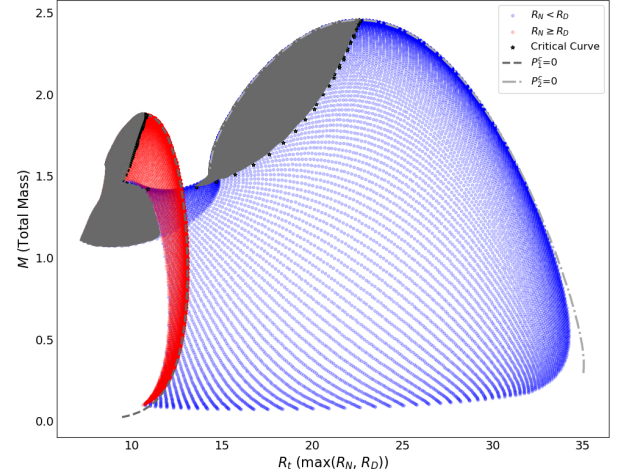


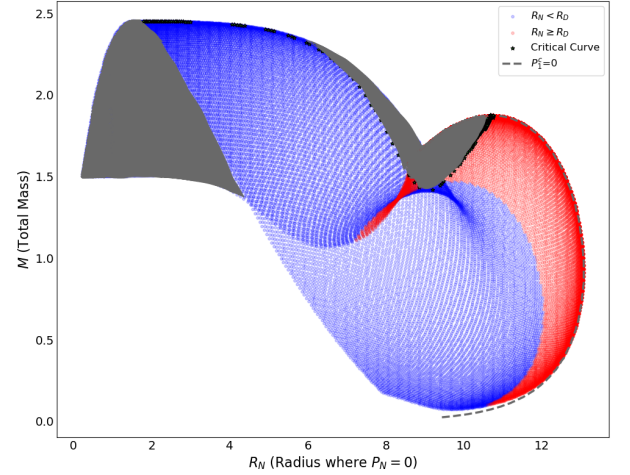
FIG. 3: Cross-validation of the stability criteria, using the same self-interacting bosonic DM and holographic NM models as in Fig.2. The plot shows the eigenvalue of the fundamental mode, ω_0^2 , calculated via the Sturm-Liouville method. The eigenvalue sign changes exactly at the critical point predicted by the static method.

This region represents the complete set of all possible observable masses and radii for stable DM-admixed NS for a given set of EoS (holographic NM EoS and self-interacting bosonic DM EoS), as shown in Fig.4. The upper panel is for M - R_t and the lower panel is for M - R_N . Here R_t is the total radius and R_N represents the radius for NM part. This has a profound observational implication: any physically realized, stable admixed star must be located within this region. In actual observations, this may not be difficult to differentiate, as electromagnetic observations see through DM and yield R_N , while observations of gravitational wave events can infer R_t through the tidal Love number [21] and mass data.

While the 2-dimensional projection onto the M - R plane is crucial for observational comparisons, it may obscure important information. There could be degeneracies that at most two different central pressure configurations result in the exact same mass and radius. This phenomenon is called “twin stars” [18, 20]. To resolve this inherent degeneracy and provide a complete topological visualization of the solution space, we introduce a third dimension to the analysis by finding a 2-dimensional surface in the 3-dimensional M - R_t - p^c space, where p^c is the central pressure of either fluid. As visualized in Fig.5, this view unfolds the stable region in the upper panel of Fig.4 into a continuous, non-overlapping surface. On this surface, each point corresponds to a unique equilibrium configuration, and different branches of solutions, including twin stars, are clearly separated. This detailed topological map is essential for unambiguously interpreting potential future observations and breaking the degeneracies inherent in simpler models.



(a) Projection onto the M - R_t plane



(b) Projection onto the M - R_N plane

FIG. 4: Projection of the stable parameter space onto the M - R_t (upper subfigure) & M - R_N (lower subfigure) plane with axes representing the total mass (in solar mass unit M_\odot) and the radius R_t, R_N (in km unit), forming a stable region. Notice that we don’t draw R_N till zero in the lower subfigure only for numerical convenience reason. The colored region represents all possible stable stars with the given set of EoS in Fig.2. The red and blue coding indicates whether the star has a DM core (red) or a DM halo (blue). The gray shaded region represents the unstable ones. The critical curve marked by green stars (\star) lies between the stable and unstable region. The dash gray line shows the M - R curve of the pure NS ($p_1^c = 0$) with holographic EoS for reference.

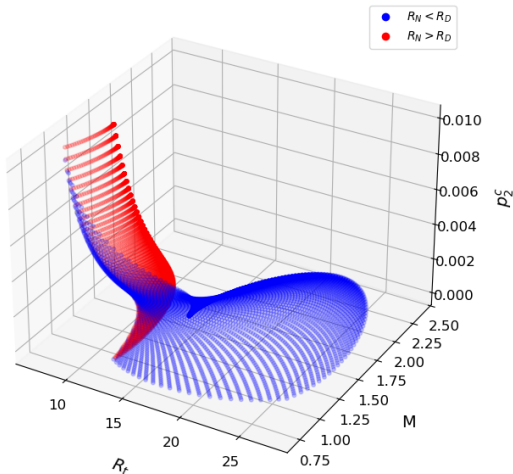


FIG. 5: The stable region in the pressure parameter space is mapped to a 3-dimensional space whose axes are total mass M (in M_\odot unit), the maximum radius $R_t = \max(R_N, R_D)$, (in km unit), and one of the central pressures (e.g., p_1^c of DM in p_\odot unit). This view resolves the degeneracies of the 2-dimensional M - R_t projection. Each point on the surface corresponds to a unique equilibrium configuration. Different branches of solutions, including “twin star” configurations, are clearly separated.

VI. COMPARISON WITH ASTROPHYSICAL OBSERVATIONS

The theoretical framework and stability analyses above provide a powerful tool for interpreting multi-messenger astronomical observations. Confronting model predictions (focusing on M - R stable region) with cutting-edge observational data enables constraining DM properties and NS EoS.

1. Key observational constraints on the NS mass-radius relation include: Mass measurements of heavy pulsars (e.g., PSR J0348+0432 [41], PSR J0740+6620 [40, 45, 46]), setting a lower bound on the maximum mass of stable compact stars;
2. Radius measurements from the NICER mission [3] (including PSR J0437-4715 [47]), providing constraints on stellar radius at specific masses;
3. Gravitational wave events from binary NS mergers (e.g., GW170817 [2, 48] and GW190425 [49]), constraining the mass-radius relation via tidal deformability (Λ).

Our admixed star model can cover a wide range of mass-radius regions by adjusting EoS parameters, and its predicted interval is consistent with the latest NICER ob-

servation of PSR J0437-4715 ($M = 1.418 \pm 0.037 M_\odot$, $R = 11.36_{-0.63}^{+0.95} km$) [47]. The model can also cover the ranges of low mass gap $3 \sim 5 M_\odot$ and high mass gap $50 \sim 100 M_\odot$, showing predictive potential for NS and certain mass gap events [35].

VII. CONCLUSION

In this work, we have addressed a foundational issue in the stability analysis of multi-fluid relativistic stars, with a specific focus on DM admixed NS. Our contributions are threefold:

First, we have presented a rigorous, step-by-step proof demonstrating the mathematical and physical equivalence of the dynamical stability criterion ($\omega_0^2 = 0$) and the static, thermodynamic criterion based on the parallelism of conserved quantity gradients ($\nabla M \parallel \nabla N_I$). This result formally validates the use of the computationally efficient static method for identifying the onset of dynamical instabilities in these complex systems.

Second, by applying this validated method, we have conducted a comprehensive and systematic stability analysis of DM-admixed NS across their entire two-dimensional parameter space. We explored various combinations of DM and NM EoS, mapping out the full topological structure of the stability boundaries. Our results confirm the existence of robust stable region and reveal non-trivial stability features that can only arise from the gravitational coupling in a multi-component system.

Third, we have translated our theoretical findings into a powerful framework for astrophysical observation. By projecting the stability regions onto the M - R plane and resolving degeneracies M - R_t - p^c diagrams, we have established a direct link between the microphysics of DM and the macroscopic, observable properties of compact stars. Our comparison with a comprehensive set of current multi-messenger data demonstrates the viability of this approach to constrain DM and NM properties, providing a solid theoretical foundation for the interpretation of future observations from next-generation GW detectors and X-ray telescopes, etc..

This work not only solidifies the theoretical underpinnings of multi-fluid mixed star stability but also provides a practical and robust toolkit for the era of precision multi-messenger astronomy, paving the way to unravel the uncertainties in NS EoS and the mystery of DM.

ACKNOWLEDGMENTS

The authors would like to thank Feng-Li Lin, Dong Lai, Qiyuan Pan, Shao-Feng Ge, Zhoujian Cao, Nobutoshi Yasutake, Chian-Shu Chen, Alessandro Parisi, Chen Zhang, Zihao Zhang, Si-Man Wu, Hao Feng and Jing-Yi Wu for helpful discussions. KZ (Hong Zhang) is supported by a classified fund from Shanghai city.

-
- [1] S. L. Shapiro and S. A. Teukolsky, *Black Holes, White Dwarfs, and Neutron Stars: The Physics of Compact Objects* (Wiley-Interscience, New York, 1983).
- [2] B. P. Abbott *et al.* (LIGO Scientific Collaboration and Virgo Collaboration), “GW170817: Observation of Gravitational Waves from a Binary Neutron Star Inspiral,” *Phys. Rev. Lett.* **119**, 161101 (2017).
- [3] K. C. Gendreau, Z. Arzumanyan, and T. Okajima, “The Neutron star Interior Composition Explorer (NICER): an Explorer mission of opportunity for the ISS,” *Proc. SPIE Int. Soc. Opt. Eng.* **8443**, 844313 (2012).
- [4] I. Goldman and S. Nussinov, “Weakly interacting massive particles and neutron stars,” *Phys. Rev. D* **40**, 3221 (1989).
- [5] C. Kouvaris, “WIMP annihilation and cooling of neutron stars,” *Phys. Rev. D* **77**, 023006 (2008).
- [6] G. Bertone and M. Fairbairn, “Compact stars as dark matter probes,” *Phys. Rev. D* **77**, 043515 (2008).
- [7] M. Deliyergiyev, A. Del Popolo, L. Tolos, M. Le Delliou, X. Lee, and F. Burgio, “Dark compact objects: An extensive overview,” *Phys. Rev. D* **99**, 063015 (2019).
- [8] V. Sagun, “Dark Matter in Neutron Stars,” *Universe* **8**, 123 (2022).
- [9] B. K. Harrison, K. S. Thorne, M. Wakano, and J. A. Wheeler, *Gravitation Theory and Gravitational Collapse* (University of Chicago Press, Chicago, 1965).
- [10] S. Chandrasekhar, “The Dynamical Instability of Gaseous Masses Approaching the Schwarzschild Limit in General Relativity,” *Astrophys. J.* **140**, 417 (1964).
- [11] F. Di Clemente, M. Mannarelli, and F. Tonelli, “Reliable description of the radial oscillations of compact stars,” *Physical Review D* **101**, 10.1103 (2020).
- [12] H. Mishra, S. Misra, P. Panda, and B. Parida, “Neutron matter-quark matter phase transition and quark star,” *International Journal of Modern Physics E* **02**, 547-563 (1993).
- [13] M. G. Alford, S. P. Harris, and P. S. Sachdeva, “On the Stability of Strange Dwarf Hybrid Stars,” *Astrophys. J.* **847**, 109 (2017), arXiv:1707.08631 [nucl-th].
- [14] D. A. Caballero, J. Ripley, and N. Yunes, “Radial Mode Stability of Two-Fluid Neutron Stars,” arXiv:2408.04701 [gr-qc].
- [15] B. Kain, “Radial oscillations and stability of multiple-fluid compact stars,” *Phys. Rev. D* **102**, 023001 (2020).
- [16] B. Kain, “Dark matter admixed neutron stars,” *Phys. Rev. D* **103**, 043009 (2021), arXiv:2102.08257 [gr-qc].
- [17] S. Valdez-Alvarado, C. Palenzuela, D. Alic, and L. A. Urena-Lopez, “Dynamical evolution of fermion-boson stars,” (2012), arXiv:1210.2299 [gr-qc].
- [18] A. Kumar and H. Sotani, “Stability analysis of two-fluid neutron stars featuring twin star and ultradense configurations,” (2025), arXiv:2509.03862 [astro-ph. HE].
- [19] A. B. Henriques, A. R. Liddle, and R. G. Moorhouse, “Stability of boson-fermion stars,” *Phys. Lett. B* **251**, 511 (1990).
- [20] M. Hippert, E. Dillingham, H. Tan, D. Curtin, J. Noronha-Hostler, and N. Yunes, “Dark Matter or Regular Matter in Neutron Stars? How to tell the difference from the coalescence of compact objects,” (2022), arXiv:2211.08590 [astro-ph. HE].
- [21] T. Hinderer, “Tidal Love numbers of neutron stars,” *Astrophys. J.* **677**, 1216-1220 (2008), arXiv:0711. 2420 [astro-ph].
- [22] S.-C. Leung, M.-C. Chu, and L.-M. Lin, “Dark matter admixed neutron stars,” *Physical Review D* **84**, 107301 (2011).
- [23] J. M. Bardeen, K. S. Thorne, and D. W. Meltzer, “A Catalogue of Methods for Studying the Normal Modes of Radial Pulsation of General-Relativistic Stellar Models,” *Astrophys. J.* **145**, 505 (1966).
- [24] R. C. Tolman, “Static Solutions of Einstein’s Field Equations for Spheres of Fluid,” *Phys. Rev.* **55**, 364 (1939).
- [25] J. R. Oppenheimer and G. M. Volkoff, “On Massive Neutron Cores,” *Phys. Rev.* **55**, 374 (1939).
- [26] Z. Rezaei, “Double dark matter admixed neutron star,” *International Journal of Modern Physics D* **27**, 1950002 (2018).
- [27] S. Mukhopadhyay, D. Atta, K. Imam, D. N. Basu, and C. Samanta, “Compact bifluid hybrid stars: hadronic matter mixed with self-interacting fermionic asymmetric dark matter,” *The European Physical Journal C* **77**, 10.1140/epjc/s10052-017-5006-3 (2017).
- [28] J. L. Friedman and B. F. Schutz, “Lagrangian perturbation theory of nonrelativistic fluids,” *Astrophys. J.* **221**, 937 (1978).
- [29] J. L. Friedman and N. Stergioulas, *Rotating Relativistic Stars* (Cambridge University Press, Cambridge, England, 2013).
- [30] X.-D. Zhou, T.-S. Chen, S.-M. W and K. Zhang, “Stability of Neutron-Dark Matter Mixed Stars and Hybrid Stars,” to appear (2025).
- [31] F. Douchin and P. Haensel, “A unified equation of state of dense matter and neutron star structure,” *Astron. Astrophys.* **380**, 151 (2001).
- [32] E. Chabanat, P. Bonche, P. Haensel, J. Meyer, and R. Schaeffer, “A skyrme parametrization from subnuclear to neutron star densities,” *Nuclear Physics A* **627**, 710 (1997). (1997).
- [33] E. Chabanat, P. Bonche, P. Haensel, J. Meyer, and R. Schaeffer, “A skyrme parametrization from subnuclear to neutron star densities part ii. nuclei far from stabilities,” *Nuclear Physics A* **635**, 231 (1998).
- [34] W. Li, J.-Y. Wu and K. Zhang, “Deriving neutron star equation of state from AdS QCD,” *Results in Physics* **64**, 107893 (2024).
- [35] K. Zhang, L.-W. Luo, J.-S. Tsao, C.-S. Chen, and F.-L. Lin, “Dark stars and gravitational waves: Topical review,” *Results in Physics*, 106967 (2023).
- [36] M. Colpi, S. L. Shapiro, and I. Wasserman, “Boson stars: Gravitational equilibria of self-interacting scalar fields,” *Physical review letters* **57**, 2485 (1986).
- [37] A. Akmal, V. R. Pandharipande, and D. G. Ravenhall, “The equation of state of nucleon matter and neutron star structure,” *Phys. Rev. C* **58**, 1804 (1998).
- [38] N. K. Glendenning and J. Schaffner-Bielich, “First-order phase transitions with more than one conserved charge: consequences for neutron stars,” *Phys. Rev. Lett.* **81**, 4564 (1998).
- [39] L. Cipriani, E. Giangrandi, V. Sagun, D. D. Doneva, and S. S. Yazadjiev, “Rapidly spinning dark matter-admixed neutron stars,” arXiv:2502.17948 [astro-ph. HE] (2025).
- [40] H. T. Cromartie *et al.*, “A very massive neutron

- star: relativistic Shapiro delay measurements of PSR J0740+6620,” *Nature Astron.* **4**, 72 (2020).
- [41] J. Antoniadis *et al.*, “A Massive Pulsar in a Compact Relativistic Binary,” *Science* **340**, 1233232 (2013).
 - [42] R. S. Lynch *et al.*, “The Green Bank Telescope 350 MHz Drift-scan Survey II: Data Analysis and the Timing of 10 New Pulsars, Including a Relativistic Binary,” *Astrophys. J.* **859**, 93 (2018).
 - [43] T. E. Riley *et al.*, “A NICER View of PSR J0030+0451: Millisecond Pulsar Parameter Estimation,” *Astrophys. J. Lett.* **887**, L21 (2019).
 - [44] M. C. Miller *et al.*, “PSR J0030+0451 Mass and Radius from NICER Data and Implications for the Equation of State of Neutron Star Matter,” *Astrophys. J. Lett.* **887**, L24 (2019).
 - [45] T. E. Riley *et al.*, “A NICER View of the Massive Pulsar PSR J0740+6620,” *Astrophys. J. Lett.* **918**, L27 (2021).
 - [46] M. C. Miller *et al.*, “The Radius of PSR J0740+6620 from NICER and XMM-Newton Data,” *Astrophys. J. Lett.* **918**, L28 (2021).
 - [47] D. Choudhury *et al.*, “A Precise NICER Radius Measurement of the Millisecond Pulsar PSR J0437-4715,” *Astrophys. J. Lett.* **971**, L20 (2024).
 - [48] B. P. Abbott *et al.* (LIGO Scientific Collaboration and Virgo Collaboration), “GW170817: Measurements of neutron star radii and equation of state,” *Phys. Rev. Lett.* **121**, 161101 (2018).
 - [49] B. P. Abbott *et al.* (LIGO Scientific Collaboration and Virgo Collaboration), “GW190425: Observation of a Binary Neutron Star Coalescence with a Total Mass $\sim 3.4M_{\odot}$,” *Astrophys. J. Lett.* **892**, L3 (2020).
 - [50] D. Kong, Y. Tian, and H. Zhang, “Dynamic and thermodynamic stability of superconducting-superfluid stars,” *arXiv:2511.03259[gr-qc]*, (2025).